Martensite and equilibrium phases in Hume-Rothery noble-metal alloys

1993 J. Phys.: Condens. Matter 5 8129

(http://iopscience.iop.org/0953-8984/5/43/024)

J. Phys.: Condens. Matter 5 (1993) 8129–8148. Printed in the UK

Martensite and equilibrium phases in Hume-Rothery noble-metal alloys

M Ahlers†‡

† Comisión Nacional de Energía Atómica, Centro Atómico Bariloche, 8400 SC de Bariloche, Río Negro, Argentina

‡ Department of Applied Physics, ETSECCIP, Universidad Politécnica de Catalunya, 08034 Barcelona, Spain

Received 23 February 1993, in final form 14 June 1993

Abstract. On the basis of recently published data for the martensitic transformations in Cu–Zn–Al alloys, an evaluation of the phase stabilities of martensitic and equilibrium phases in other noble-metal alloys has been made. The contributions which control the Gibbs energy of the different phases are discussed quantitatively. The most important of these are the stability of the disordered phases, the vibrational entropy, the influence of the long-range order characterized by pair interchange energies, the structure-dependent lattice distortions and the energies associated with the stacking sequences in the different close-packed phases.

1. Introduction

The noble-metal alloys of Cu, Ag and Au with subgroup B elements form a rather coherent group as concerns the temperature and composition ranges of the different equilibrium phases [1]. Their stabilities seem to be controlled mainly by the electron concentration e/a. This has been taken as evidence that the interaction of the non-localized s- and p-electron states at the Fermi surface with the structure-dependent Brillouin zone boundaries determines the selection of the different phases. Doubts arose when it became apparent that the Fermi surface touches the Brillouin zone already in pure copper. In addition, long-range order is often observed whose Gibbs energy contribution can exceed considerably that between the different phases. Although repeated efforts have been made to evaluate theoretically the relative stabilities of the different phases, it is extremely difficult to determine the enthalpy and entropy differences experimentally, first because they are so small and second because they can be influenced by short-range order effects which are difficult to quantify.

In this respect the martensitic transformations in the noble-metal alloys are a great help. Although martensite is a non-equilibrium structure, it permits one also to deduce information on the equilibrium phases [2]. This is because the enthalpy and entropy differences involved in a martensitic transformation can be measured experimentally with the required precision, and because there is no change in configurational entropy, since the martensitic transformation is diffusionless, without a change in the atom distribution on the lattice sites.

Recently an experimental study of the martensitic transformations in Cu–Zn and Cu–Zn–Al alloys has been completed and the factors which contribute to their stability have been analysed quantitatively [3–5]. They include the long-range order contribution, the influence of the different stackings of the close-packed martensites and the lattice parameter changes.

0953-8984/93/438129+20$07.50

It seems appropriate now to apply these concepts to other noble-metal alloys, for which considerable experimental information exists, although not that detailed [6, 7]. In this paper the face-centred ordered martensites and their relationship with the disordered α-phase solid solutions, and the hexagonal martensitic and equilibrium structures, will be mainly discussed. Although the Ni–Al alloys do not belong to the noble-metal alloys, their martensites are similar, which warrants a brief consideration also of this system.

2. Martensite and equilibrium structures based on the FCC lattice

2.1. Face-centred martensites and the contribution of long-range order

Face-centred martensite is generally observed for the lowest electron concentrations at which the BCC phase is stable at high temperatures. The high-temperature β-phase from which it forms can be disordered prior to the transformation (denoted A2 or β) or it can have order in first neighbours (B2 or β_2), or also in second neighbours ($D0_3$ or β_1, and $L2_1$ or β_3). Face-centred martensite is denoted 3R, if disorder or B2 order is inherited, and 6R for $D0_3$ or $L2_1$ order [2]. In $L2_1$ ordered Cu–Zn–Al alloys with $e/a \simeq 1.48$ the 6R martensite is nearly cubic with a small tetragonal distortion at $c/a \simeq 0.985$ [5]. This justifies considering the 6R simply as a face-centred structure onto which order is imposed, which is described in terms of pair interchange energies whose composition dependence is neglected. This approach will also be adopted for the other noble-metal alloys.

Most order–disorder descriptions limit themselves to only first- and second-neighbour interactions, $i = 1, 2$:

$$w_{AB}^{(i)} = -2V_{AB}^{(i)} + V_{AA}^{(i)} + V_{BB}^{(i)} \tag{1}$$

where the $V_{AB}^{(i)}$ are the interaction energies between the corresponding atoms on a given Bravais lattice. In the following, w represents the pair interchange energies in the high-temperature β-phase, and m those in the martensites. In the high-temperature phase, based on the BCC Bravais lattice, the state of order is described by the occupation probabilities p_A^J of atoms A on the four sublattices J ≡ I–IV (figure 1). For B2 order, $p_A^I = p_A^{II} \neq p_A^{III} = p_A^{IV}$; for $D0_3$ order, $p_A^I = p_A^{II} = p_A^{III} \neq p_A^{IV}$; for $L2_1$ order, $p_A^I = p_A^{II} \neq p_A^{III} \neq p_A^{IV}$. It is convenient to introduce as a measure of B2 order the quantity

$$x_A = \tfrac{1}{4}(p_A^I + p_A^{II} - p_A^{III} - p_A^{IV}). \tag{2}$$

In the presence of $D0_3$ or $L2_1$ order an additional parameter

$$z_A = \tfrac{1}{2}(p_A^{III} - p_A^{IV}) \tag{3}$$

is required [12]. If the maximum degree of long-range order prior to the transformation is reached, then the order parameters are related to the composition of a ternary system by

$$\begin{aligned} x_A &= 1 - c_A \qquad x_B = -c_B \qquad x_C = -c_C \\ z_A &= 2c_A - 1 \qquad z_C = -2c_C \qquad z_A + z_B + z_C = 0 \end{aligned} \tag{4}$$

where A denotes the majority atom with $c_A \geqslant 0.5$, $w_{AC}^{(2)} > w_{AB}^{(2)}$, and the c_A are the atomic fractions. This corresponds to the configuration with the lowest energy, with all C atoms but no A atom on sublattice IV, and the B atoms distributed on III and IV sites. Since the

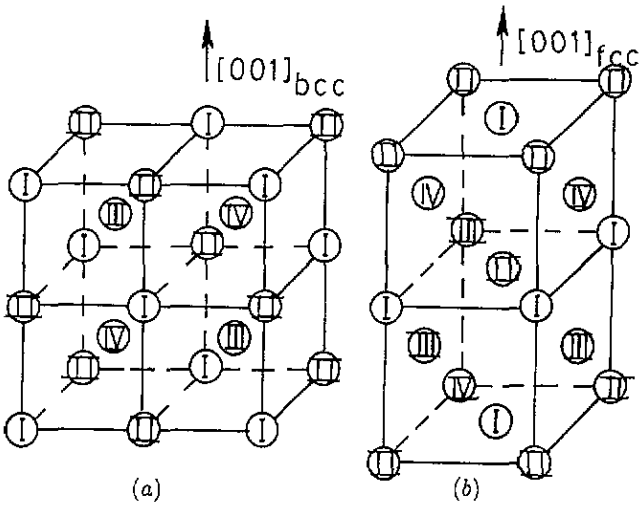

Figure 1. (*a*) Four BCC unit cells with the four different sublattice sites. (*b*) Two FCC unit cells with the sublattice sites inherited from the BCC structure.

martensitic transformation proceeds generally at low temperatures, it is possible to obtain the maximum degree of long-range order in the BCC phase by careful previous heat treatments, as discussed for Cu–Zn–Al alloys [8, 9].

The ordering energies can be evaluated straightforwardly for the ordered BCC and the order-inherited FCC phase. In the B2 lattice (figure 1(*a*)), each atom on the (I+II) sublattices has eight nearest neighbours on the other (III+IV) sublattices, and vice versa. The six second-nearest neighbours lie on the same sublattice pair set (I+II) or (III+IV). If A–B bonds are favoured, $w_{AB}^{(i)} > 0$, then the first-neighbour pairs contribute favourably, and the second-neighbour pairs unfavourably. Third- and higher-order pair interchange energies are generally assumed to be small and therefore are neglected. The enthalpy of formation of the B2 ordered BCC phase is therefore

$$H_{B2}^{\beta} = H_{dis}^{\beta} + \tfrac{1}{2}\sum_{A,B}(8w_{AB}^{(1)} - 6w_{AB}^{(2)})x_A x_B \tag{5}$$

where the sum is over the different atom pairs. The factor of $\frac{1}{2}$ in front of the sum avoids the double counting of pairs (see also [2]).

During the martensitic transformation the B2 structure is changed to $L1_0$ (figure 1(*b*)). An atom now has 12 first neighbours, of which four lie on the same set (I+II) or (III+IV), and eight on different sets, so that only four favourable net first-neighbour bonds remain. The six next-neighbour pairs lie always on the same unfavourable (I+II) or (III+IV) set. Thus, for the FCC (α) martensite with B2 inherited order, the enthalpy of formation is [2]

$$H_{B2}^{\alpha} = H_{dis}^{\alpha} + \tfrac{1}{2}\sum_{A,B}(4m_{AB}^{(1)} - 6m_{AB}^{(2)})x_A x_B. \tag{6}$$

When $D0_3$ or $L2_1$ order is present in the BCC phase, then each sublattice III site has six favourable sublattice IV sites as next-nearest neighbours. After the transformation this leads to four favourable III–IV first-neighbour pairs and to four unfavourable III–III and IV–IV

second-neighbour pairs on the same (001) plane, in addition to two favourable III–IV pairs on neighbouring (001) planes. Thus the change in enthalpy difference, when $L2_1$ order is added to B2, becomes [2, 10]

$$(H^{\beta}_{L2_1} - H^{\beta}_{B2}) - (H^{\alpha}_{L2_1} - H^{\alpha}_{B2}) = \tfrac{1}{4}\sum_{A,B}[6w^{(2)}_{AB} - (4m^{(1)}_{AB} - 2m^{(2)}_{AB})]z_A z_B. \quad (7)$$

The factor $\frac{1}{4}$ takes care of the single counting and of the ordering in only a half of all sublattice sites, i.e. those corresponding to III and IV. It should be noted that the martensite with a $D0_3$ inherited order does not lead to the commonly observed $L1_2$ Cu_3Au-type order, but to $D0_{22}$.

The enthalpy difference between the ordered BCC and the corresponding FCC phase can be determined experimentally, according to

$$H^{\beta}_{L2_1} - H^{\alpha}_{L2_1} = T_0\,\Delta S. \quad (8)$$

In the noble-metal alloys the hysteresis is small between the starting temperature M_s for the martensite transformation on cooling and the temperature A_f of the end of the retransformation, being of the order of 10 K. The temperature T_0 is expected to lie in between these limits, $M_s < T_0 < A_f$, but owing to the scatter from sample to sample no error is committed by setting $T_0 \simeq M_s$. The entropy difference ΔS is due solely to the change in vibrational modes, since the configurational entropy does not change, and the density of electronic states at the Fermi surface is too small to be of importance. (The difference between the electronic specific heats of the phases is considerably smaller than that of the FCC alloys, which amounts to $\gamma = 0.8$ mJ mol^{-1} T^{-2} [78]. Therefore, the contribution to ΔS from the conduction electrons is far below $\gamma T = 0.03k_B$ at room temperature.) It has been shown [11] that it is the soft $\{110\}_\beta\langle 1\bar{1}0\rangle_\beta$ transverse modes in the BCC phase which are mainly responsible for ΔS, as had been proposed originally by Zener [77]. ΔS depends only weakly on alloy composition in the Cu–Zn–Al systems, according to [3]

$$\Delta S = [0.51(e/a) - 0.58]k_B. \quad (9)$$

ΔS is, within experimental scatter, the same for B2 and $L2_1$ order and does not change when the transformation proceeds to martensites with different stacking sequences, as 9R, 18R or 2H. Thus an equivalent to equation (8) holds also for B2 ordered martensitic transformations, and for transformations to differently stacked martensites, with the same ΔS from equation (9).

If the pair interchange energies for the β-phase and the martensite can be determined, then it is possible to obtain the enthalpy difference between the disordered FCC α- and BCC β-phases by subtracting from the measured enthalpy difference (equation (8)) the long-range order contribution according to equations (5)–(7).

The pair interchange energies can be determined in several ways.

(a) They can be found from the critical ordering temperatures. For a binary A–B alloy around an equiatomic composition with B2 order, the relationship between the critical temperature T^{β}_c for B2 ordering at $c_A = 0.5$ and the pair interchange energies can be expressed as

$$4w^{(1)}_{AB} - 3w^{(2)}_{AB} = \beta_0 T^{\beta}_c. \quad (10)$$

β_0 depends on the ratio $w^{(2)}_{AB}/w^{(1)}_{AB}$. Inden [12] writes $\beta_0 = 2/\kappa$ and presents the relationship between $w^{(2)}_{AB}/w^{(1)}_{AB}$ and κ, as obtained by comparing the results from the simple Bragg–Williams–Gorski (BWG) theory ($\kappa = 1$) with those from the cluster variation method. For Cu–Zn with $w^{(2)}_{CuZn}/w^{(1)}_{CuZn} = 0.56$ (table 1), $\beta_0 = 3.00$ is derived and, for Cu–Al ($w^{(2)}_{CuAl}/w^{(1)}_{CuAl} = 0.61$) (table 1), $\beta_0 = 3.26$ would be appropriate. The ratio $w^{(2)}_{AB}/w^{(1)}_{AB}$ has to be deduced from additional experimental information, e.g. from the critical $L2_1$ ordering temperature in ternary alloys. For those binary alloy systems whose $w^{(2)}_{AB}/w^{(1)}_{AB}$ is not known experimentally, an average $\beta_0 = 3.1$ will be used in the following.

For face-centred alloys with $c_B \simeq 0.25$, ordering in first- and second-nearest neighbours leads to an $L1_2$ ground structure, if $m^{(2)}_{AB}/m^{(1)}_{AB} < 0$ and to $D0_{22}$ for $0 < m^{(2)}_{AB}/m^{(1)}_{AB} < 0.5$ [13]. In some α-phase noble metals, ordering is accompanied by the formation of long-period superlattice structures, which can be described by a mixture of $L1_2$ and $D0_{22}$ on an atomic scale. This makes it difficult to determine experimentally the sign of $m^{(2)}_{AB}$ but indicates that $m^{(2)}_{AB}$ is small compared with $m^{(1)}_{AB}$, since otherwise either $D0_{22}$ or $L1_2$ would be stable also at finite temperatures. The relationship between the critical ordering temperature at $c_B = 0.25$ and the first- and second-neighbour pair interchange energies in the FCC lattice can be written as

$$2m^{(1)}_{AB} - 3m^{(2)}_{AB} = \alpha_0 T^{\alpha}_c. \tag{11}$$

For $m^{(2)}_{AB} = 0$, α_0 is found to be 4.30 both from the cluster variation method and from Monte Carlo calculations [13]. In the following this value for α_0 will be used for an approximate evaluation of $m^{(i)}_{AB}$ from T^{α}_c, whenever available. Following other workers (see, e.g., [12]), the pair interchange energies are expressed here in units of the Boltzmann constant and thus have the dimension of temperature. In order to transform them into joules per mole, they have to be multiplied by 8.3143 J mol^{-1} K^{-1}.

(b) The pair interchange energies can also be estimated from an analysis of the influence of the $L2_1$ order on the martensitic transformation temperature M_s, according to equation (7). This requires, on the one hand, that crystals with perfect B2 and $L2_1$ order can be obtained by a careful and appropriate pre-treatment and, on the other hand, that no other contribution influences the energy difference between the B2 and $L2_1$ ordered crystals. Both conditions are met in the Cu–Zn–Al system [3, 9]. In these alloys it is the 9R or 18R martensite that is most commonly observed but, since the energy difference between the FCC and the 9R or 18R martensite is independent of the second-neighbour ordering in β [4], the relationship of equation (7) can also be applied to these martensitic structures. For the other noble-metal alloy systems, no experimental verification exists yet. Nevertheless it will be assumed for the following that the relationship holds also for the other alloys.

(c) Pair interchange energies have also been determined from the diffuse scattering of short-range-ordered alloys. This method is quite elaborate, and a wide variety of values can be obtained [14], unless very careful experimental measurements are made, as in the case of Cu–Zn [15]. In the latter case it has been shown that the pair interchange energies from short-range order in Cu–31.1 at.% Zn agree well with those deduced from the change in M_s between B2 and $L2_1$ order [3].

2.2. Martensite in the Cu–Zn–Al alloys

This system has been discussed in detail elsewhere [3–5]. Therefore, only a few aspects of relevance in comparison with other noble-metal alloys will be presented. The martensite that is generally observed does not have the face-centred structure but contains stacking

Table 1. Data for noble-metal alloys. To obtain the energies (which in this table are expressed in kelvins) in joules per mole, they should be multiplied by 8.3143 J mol^{-1} K^{-1}.

(1) System	(2) $w^{(1)}_{AB}$ (K)	(3) $w^{(2)}_{AB}$ (K)	(4) $\frac{3}{2}w^{(2)} - m^{(1)} + \frac{1}{2}m^{(2)}$ (K)	(5) $m^{(1)} - \frac{1}{2}m^{(2)}$ (K)	(6) $m^{(1)} - \frac{3}{2}m^{(2)}$ (K)	(7) T_c^{α} (experimental) (K)	(8) T_c^{α} (calculated) (K)	(9) $\frac{1}{6}A^{\alpha}_{dis}$ (K)	(10) c_B (at.%)
Cu–Zn	955	535[a]	+290[b]	512[c]			238[d]	785	50[e,f]
Cu–Al	1345	825[g]	−275[b]	1512[c]		(636)[h]	703[i]	1536	18.5[e]
Cu–Ga	(1345)	(825)[j]						305	8[e]
Cu–Sn	> 1370	> 800[k]			710 ± 150[m]		330 ± 70[i]	648	43[e]
Ag–Cd	810 ± 130	445 ± 70[l]			(473)[n]		(220)[i]	427	34[e]
Ag–Zn	585	300[a]						388	20[e]
Ag–Al	—	—			1436[n]	668[p]		1235	28.5[e]
Ag–Mg	> 1500	> 870[o]			⩾ 1480[m]	⩾ 690[p]		1457	24[e]
Au–Cd	> 1240	> 718[q]			1490[m]	693[p]		1600	25[e]
Au–Zn	1785	1000[a]						370	50[e]
Au–Ag	455	535[a]					328[i]	370	50[e]
Au–Ag		470[r]	≃ 0[s]	705[c]			602[i]	411	50[e]
Au–Cu	1210	660[a]	−305[t]	1295[c]	1425	663[p]			

[a] From [17]. [b] From [3]. [c] From columns (3) and (4). [d] Neglecting the difference between $m^{(1)} - \frac{1}{2}m^{(2)}$ and $m^{(1)} - \frac{3}{2}m^{(2)}$, calculated with $\alpha_0 = 4.3$. This calculated T_c^{α} agrees with that deduced from *ab-initio* calculations by Turchi *et al* [16]. [e] From mixing enthalpies measured at the alloying concentration c_B [52, 53] and corrected with the enthalpy differences between FCC and hexagonal Zn (274 K), Cd (231 K) and Mg (234 K) [54]. [f] From [2]. [g] From Cu–Zn–Al at $e/a = 1.48$ [74]. [h] From the peritectic temperature below which the ordered α_2-phase is observed in Cu–Al [52]. [i] Calculated from column (5) with $\alpha_0 = 4.3$ and $\frac{3}{2}m^{(2)} \simeq \frac{1}{2}m^{(2)}$. [j] From the similarity of the B_2 ordering temperatures of Cu–Al and Cu–Ga. [k] From the $D0_3$ ordering temperature of 1000 K at 14.8 at.% Sn [46], taking $T_c^{\beta} > 1000$ K and assuming that $\beta_0 = 3.1$ and $w^{(2)}/w^{(1)} = 0.58$. [l] Taking $T_c^{\beta} = 613 \pm 100$ K (corresponding to the middle of the range between the possible upper and lower limits for T_c^{β}), $\beta_0 = 3.1$ and $w^{(2)}/w^{(1)} = 0.55$. [m] From the experimental T_c^{α} and $\alpha_0 = 4.3$. [n] From $T_0 - M_s$ and columns (2) and (3). [o] From $T_c^{\beta} > 1093$ K, $\beta_0 = 3.1$ and $w^{(2)}/w^{(1)} = 0.58$. [p] Critical ordering temperatures for the binary alloys at 25 at.% and identified with T_c^{α} [52]. [q] From $T_c^{\beta} > 902$ K, $\beta_0 = 3.1$ and $w^{(2)}/w^{(1)} = 0.58$. [r] From the $L2_1$ ordering temperature in Ag–Au–Cd according to [41]. [s] Based on data of Nakanishi *et al* [42] for Ag–Au–Cd. [t] From data for Cu–Zn–Au [10].

faults on each third close-packed plane. Their contribution to the energy has been evaluated [4] and, by subtracting it, the enthalpy difference between the high-temperature phase and the face-centred martensite could be deduced. The pair interchange energies for the β-phase were determined from the critical B2 and $L2_1$ ordering temperatures and are listed in table 1. From the influence of $L2_1$ order on the martensitic transformation the values of $m^{(1)}_{AB} - \frac{1}{2}m^{(2)}_{AB}$ were derived for the Cu–Zn and Cu–Al pairs [3]. In α-phase Cu–Zn, no long-range order is observed, but the pair interchange energies deduced from the short-range order [15] are in good agreement. In Cu–Al an intermediate long-range-ordered face-centred phase is present at around 23 at.% Al. If its decomposition temperature is identified with the critical ordering temperature, $m^{(1)}_{CuAl} - \frac{3}{2}m^{(2)}_{CuAl} = 1376$ K is derived according to equation (11), in rather good agreement with $m^{(1)}_{CuAl} - \frac{1}{2}m^{(2)}_{CuAl} = 1512$ K, taking into consideration the uncertainties in $m^{(2)}_{CuAl}$.

By subtracting the long-range order contribution from the enthalpy difference in the martensitic transformation, the enthalpy difference between the perfectly disordered FCC and BCC structures has been obtained [5]. For Cu–Zn the result agrees well with *ab-initio* calculations [16]. For Cu–Al, no such data are available. For the BCC disordered Cu–Zn the enthalpy of formation can be adjusted by a parabola with a constant coefficient, only if it is assumed that BCC Zn is more stable than FCC Zn.

The enthalpy differences between the disordered α and β should also be compared with the α–β-phase boundary of the equilibrium phase diagrams. The enthalpy differences [5] can be expressed by

$$H^{\beta}_{dis} - H^{\alpha}_{dis} = 372 - 555c_{Zn} \qquad \text{for Cu–Zn} \tag{12}$$

$$H^{\beta}_{dis} - H^{\alpha}_{dis} = 514 - 2060c_{Al} \qquad \text{for Cu–Al.} \tag{13}$$

For Cu–Al the second-neighbour contribution $m^{(2)}_{CuAl}$ is neglected. The peritectic temperature between the liquid, α and β is the highest equilibrium temperature between α and β for which short-range order effects play the smallest role. On the assumptions that the Gibbs energies of α and β are the same in the middle of the two-phase region, and that equations (12) and (13) are valid also at these high temperatures, the corresponding entropy difference can be derived. For Cu–34 at.% Zn at the peritectic temperature of 1176 K, $\Delta S = 0.154k_B$ and, for Cu–17.9 at.% Al at 1310 K, $\Delta S = 0.111k_B$ is deduced. For Cu–Al, this ΔS agrees quantitatively with the value which is expected from the martensitic transformation (equation (9)). For Cu–Zn there exists a difference. This is at least in part due to some short-range disorder which is retained even at high temperatures and stabilizes the β-phase. Owing to the large difference in the critical order temperatures, its influence in α is smaller, and thus the two-phase α–β boundary is shifted to lower values. If equation (9) for ΔS and equation (12) for $H^{\beta}_{dis} - H^{\alpha}_{dis}$ are valid, the two-phase region has to be shifted by 5 at.% Zn to higher values in the absence of short-range order contributions. This brings it close to the same electron concentration as for the Cu–Al system, and emphasizes again the predominant role of the electron concentration although strong Fermi surface–Brillouin zone interactions especially in this composition range are absent in the α-phase.

2.3. Martensite in the Cu–Au–Zn alloys

The binary Au–Zn alloys present some peculiarities that are absent in Cu–Zn–Al. The β-phase is ordered to the melting point. The critical ordering temperature has been estimated as 1386 K for 50 at.% Zn, by extrapolating from ternary alloys [17]. At around 37.5 at.%

Zn a stable phase with an order different from B2 but based on the BCC has been observed [18]. This indicates that the atom distribution can be more complex than that of an ideal B2 structure at the equiatomic composition if the order energy is high.

A martensitic transformation has been observed for Au–Zn alloys with a zinc content above 46 at.%, whose M_s increases with increasing zinc concentration [19,20], and is modified by the cooling conditions in the high-temperature phase.

In the α-phase solid solution, several long-period superlattice structures are observed [18,21]. At 25 at.% Zn ordering to an $L1_2$ structure with antiphase boundaries (APBs) on (100) planes, two unit-cell distances apart, occurs at a temperature of 693 K. This APB formation may be an indication that $m^{(2)}_{AuZn}$ is small. This temperature leads to an energy of (equation (11)) $m^{(1)}_{AuZn} - \frac{3}{2}m^{(2)}_{AuZn} = 1490$ K. The order contribution increases the stability of the BCC phase more than that of the FCC martensite (equations (5) and (6)). For an alloy concentration $c_{Zn} = 0.40$ the BCC is favoured by an energy of 210 K, which implies a lowering in M_s with respect to the hypothetical disordered phases of about 1000 K (using a reasonable upper limit value for $\Delta S = 0.2k_B$). Thus, the failure to observe a martensitic transformation below 46 at.% Zn can be rationalized. The reason for the appearance of the martensite above this Zn concentration and its anomalous increase with increasing c_{Zn} into the range of major stability of the equilibrium B2 phase is not understood.

In the ternary Cu–Au–Zn alloys with Au concentrations of around 25 at.% and c_{Zn} of between 0.45 and 0.50, $L2_1$ order has been observed for the β-phase. From the critical B2 and $L2_1$ order temperatures the pair interchange energies of the Cu–Au pairs in the BCC lattice were derived [17] (see table 1). The $L2_1$ order is associated with an increase in M_s [22–24]. From the temperature dependence of the critical stress to induce martensite above M_s in Cu–Au–Zn alloys with 26 at.% Au and 45–49 at.% Zn reported by Miura *et al* [25], an entropy change $\Delta S = (0.21 \pm 0.01)k_B$ was deduced [10]. If equation (9) were valid, $\Delta S = 0.175k_B$ would be expected for $e/a = 1.48$, which within the experimental scatter is quite similar. An analysis of the $L2_1$ dependence of M_s according to equation (7) [10] permits one to obtain $m^{(1)}_{CuAu} - \frac{1}{2}m^{(2)}_{CuAu} = 1295$ K. It is interesting to compare this value with that obtained from the critical ordering temperature $T_c = 663$ K in the binary FCC Cu_3Au alloy. According to equation (11), $m^{(1)}_{CuAu} - \frac{3}{2}m^{(2)}_{CuAu} = 1425$ K, a value which is very close to that derived here, in spite of the differences in the electron concentrations of the alloys, in the type of order, in the lattice parameter and in the uncertainty of the value for $m^{(2)}_{CuAu}$.

2.4. Martensite in the Ag–Au–Zn alloys

In the binary Ag–Zn alloys the BCC equilibrium phase is disordered and is replaced by the ξ-phase below 547 K. The B2 ordering temperature was deduced by extrapolating results from ternary $Au_cAg_{0.5-c}Zn_{0.5}$ alloys [26], and $T_c^\beta = 506$ K was obtained for Ag–50 at.% Zn [17]. Iwasaki *et al* [27] measured the pressure dependence of the ordering temperature for Ag–50.4 at.% Zn. By linear extrapolation to atmospheric pressure an ordering temperature of 495 K is derived, in good agreement with the former value. The critical ordering temperatures in the Ag–Au–Zn β-phase alloys permitted also the interchange energies of the Ag–Au pairs in the BCC structure to be derived [17]. They are listed in table 1. In the α-Ag–Zn alloys, no long-range order has been observed.

A martensitic transformation has been found and analysed for Ag–38 at.% Zn, with an M_s of 133 K [28]. The martensite plates consist of a 3R and a 9R structure, which is an indication that they have nearly the same enthalpy of formation. From M_s and the pair interchange energies in the β-phase it is possible to estimate the critical ordering temperature and the corresponding pair interchange energies in the FCC α-phase. This is done in the

following way. Since the ordering temperatures in the α- and the β-phases are low, it can be expected that the location of the $\alpha + \beta$ two-phase region in the phase diagram is not modified by short-range order at high temperatures and that therefore the temperature in the middle of the two-phase region is a good approximation for the α–β temperature T_0. By linear extrapolation to 38 at.%, $T_0 = 860$ K is obtained. Thus the difference $T_0 - M_s$ is due to the order contribution in the martensitic transformation. Knowing the β-phase order energy (equation (10)) and using the same entropy difference as for Cu–Zn–Al (equation (9)) ($\Delta S = 0.124 k_B$), a critical ordering temperature for the FCC phase of $T_c^\alpha = 220$ K, and an energy of $m_{AgZn}^{(1)} - \frac{3}{2} m_{AgZn}^{(2)} = 473$ K is obtained. This T_c^α is very reasonable, taking into consideration that, in α-Ag–Zn, no long-range order but considerable short-range order has been found [29], similar to that in α-Cu–Zn and α-Cu–Al of approximately the same e/a [30].

In the ternary $Au_cAg_{0.5-c}Zn_{0.5}$ alloys with around 25 at.% Au the critical $L2_1$ order temperature is increased. In the Cu–Au–Zn system this is associated with a considerable shift in M_s to higher temperatures. A similar influence of $L2_1$ order on M_s is unlikely for the Au–Ag–Zn alloys because, as will be discussed, the influence of $L2_1$ order is small for the Ag–Au–Cd alloys around the $AgAuCd_2$ composition at which only the Ag–Au pairs contribute, as in Ag–Au–Zn.

2.5. Martensite in the Ag–Au–Cd alloys

Apart from the Cu–Zn- and Cu–Al-based alloys it is the Au–Cd system whose martensitic transformation has been studied in most detail. The binary Au–Cd BCC phase is ordered to the melting point [31], and its critical ordering temperature is not known. In the α-phase, some ordered structures are observed [32, 33] which are not only peaked at 25 at.% Cd but extend as long-period superlattices to higher concentrations. Therefore the simple cluster variation approximation which leads to equation (11), probably is not valid. An evaluation of the martensitic transformation in terms of the long-range order contribution, as done for the other alloys, therefore is not justified at this stage. Moreover, the martensite has a strongly distorted 9R structure, and its M_s is modified considerably by the quenching conditions [34], which would not be expected from the high ordering temperature in the β-phase, unless more complex order patterns are present, as in the case of the Au–Zn system at around 37.5 at.% Zn. The high M_s are not incompatible, however, with the high ordering tendencies in the α- and β-phases.

In the binary Ag–Cd alloys the disordered BCC is separated from the B2 ordered β'-phase by a hexagonal ξ-phase field which extends from 513 to 713 K. The critical B2 ordering temperature lies within this range. As a first approximation it will be positioned in the middle at $T_c^{B2} = 613$ K. This temperature is sufficiently high for ordering to occur during the quench as in Cu–Zn–Al with $L2_1$ order for quenches above 600 K [9]. On the other hand it is low enough that ordering remains incomplete when the hexagonal ξ-phase becomes sufficiently stable (see below for a more detailed justification).

In α-Ag–Cd only short-range order has been observed [35]. Since, therefore, T_c^α is not available, we shall attempt to determine it from the martensitic transformation, as has been done for Ag–Zn. The temperatures M_s as reported in three different papers [36–38] agree quite closely, which supports the observation that in Ag–48.3 at.% Cd the order is perfect, even after quenching [39]. The Cd concentration dependence of M_s can be expressed as

$$M_s\,(\mathrm{K}) = 1560 - 3008 c_{Cd}. \tag{14}$$

The martensite has 9R and 2H structures [40] and not the face-centred lattice as supposed for the present discussion, but this difference will be neglected considering the uncertainty

in T_c^β. Using linear extrapolation from high temperatures of T_0 in the middle of the two-phase region, and ΔS from equation (9), $T_c^\alpha = 330$ K is obtained if it is assumed that $T_c^\beta = 613$ K. It would change by ± 70 K, if the upper and lower limits for T_c^β were taken. The corresponding pair interchange energies for the BCC and FCC phases are listed in table 1 with their upper and lower limits. In order to derive $w_{AgCd}^{(i)}$ a ratio $w_{AgCd}^{(2)}/w_{AgCd}^{(1)} = 0.55$ has been used.

Ternary Ag–Au–Cd alloys with Ag concentrations of around 25 at.% have been analysed for the critical $L2_1$ ordering temperature and for the martensitic transformation [41, 42]. From the critical temperature for $L2_1$ ordering, $T_c^{L2_1} = 474$ K for 20 at.% Au–30 at.% Ag–50 at.% Cd alloy, $w_{AgAu}^{(2)} = 470$ K is derived, supposing perfect B2 order prior to the $L2_1$ ordering. This value is smaller than that obtained from the Ag–Au–Zn alloys by Inden [17], who considered incomplete B2 order, according to the BWG model. If perfect order is assumed, his value shifts from 535 K by only a small amount to 570 K. It is possible that the difference between the lattice parameters of Ag–Au–Cd and Ag–Au–Zn [42] is the reason for the difference in $w_{AgAu}^{(2)}$.

By quenching, the $L2_1$ order can be suppressed [42]. There is, however, hardly any influence on M_s, which is lowered by only a few kelvins. According to equation (7), this implies that $m_{AgAu}^{(1)} - \frac{1}{2}m_{AgAu}^{(2)} = \frac{3}{2}w_{AgAu}^{(2)} = 700$ K. If the second-neighbour contribution $m_{AgAu}^{(2)}$ can be neglected, and if extrapolation to binary Ag–Au is permitted, a critical ordering temperature $T_c^\alpha = 325$ K is expected according to equation (11). This value relates favourably to the strong short-range order or even small-particle long-range order after irradiation at 55 °C in 50 at.% Au alloys [43].

2.6. Binary noble-metal alloys with subgroup B elements whose valency is higher than two

The alloy systems that will be discussed are Cu–Ga, Cu–Sn and Ag–Al, since for them information on the martensitic transformation is available. Existing results for ternary alloys for which the third component is present in small quantities of less than 5 at.% will not be considered here, because without additional information on the influence of α–β-phase stability, on the atom distribution between the lattice sites and on the change in β-phase order energy, the interpretation remains highly speculative.

The Cu–Ga alloys resemble in many respects the Cu–Al alloys. On quenching, the β-phase orders below the β-phase stability range at temperatures which are equal to those in Cu–Al [44]. At the lowest Ga content, M_s lies above T_c^β, and a disordered martensite forms. M_s coincides well with the extrapolated T_0 in the middle of the $\alpha + \beta$ two-phase region, as in Cu–Al [45]. Apparently the short-range order which exists above M_s does not modify M_s. This indicates that the inherited short-range order in the α-phase modifies the stability in the same way as in β. If we take the short-range order energy proportional to that for long-range order, this implies that $\beta_0 T_c^\beta \simeq \alpha_0 T_c^\alpha$, a relation that is obeyed for Cu–Al, according to the pair interchange energies derived for that system. It is therefore concluded that the pair interchange energies for the α- and β-phases in Cu–Ga are essentially the same as for Cu–Al.

The β-phase in Cu–Sn seems to order at a high temperature between 1000 and 1025 K, in spite of the low Sn concentration of 14.8 at.%, at which the β-phase is stable [46]. This is an indication that the Cu–Sn pair interchange energy for the β-phase is high. The temperatures M_s have been measured [47]; they depend on the pre-treatment in the β-phase and on the aging in the martensite. The relationship between M_s and T_0 in the middle of the $\alpha + \beta$ two-phase region cannot be determined with the required precision, since the $\alpha + \beta$ two-phase region has a wide composition range and a narrow temperature range. If

the temperatures in the middle of the $(\alpha + \beta)$-phase are extrapolated to the composition for which the martensitic transformation is observed, $M_s = 460$ K would be expected, compared with the observed value of 210 K. This difference between T_0 and M_s, if it is real, is an indication that the long-range order stabilizes the β-phase more than the α-phase.

In β-Ag–Al, no long-range order has been observed after quenching [48]. It would be expected therefore that, similar to Cu–Al and Cu–Ga at the lowest electron concentration, the temperatures M_s coincide with the extrapolated temperatures T_0 in the middle of the $\alpha + \beta$ two-phase region. Probably this was the argument which led Arias and Kittl [49] to estimate M_s. The measured temperatures M_s [50] are considerably lower; instead of 660 K, M_s is 170 K for 25 at.% Al. This large difference could be rationalized as being due to the short-range order energy in the β-phase, if the corresponding energy contribution in the α-phase were negligible. Experimental results [51] have established the existence of short-range order; therefore the reason for the low M_s is not clear. It should be remarked, however, that in Ag–Al alloys a massive transformation occurs even during quenching [49], and maybe the depression in M_s is also related to it.

2.7. The stability of the FCC and BCC equilibrium phases in the noble-metal alloys: a comparison

The stability of the Hume-Rothery phases has been discussed in terms of three variables, namely the lattice parameters, the electron concentration and the electronegativity [1]. In the cubic α- and β-phases the atomic volume is the same and, since it determines the distances between the atoms, the lattice parameters are not a free variable to adjust the enthalpy difference between α and β, in contrast with the hexagonal phases to be discussed below.

The electronegativity is generally described in terms of pair interchange energies. The long-range order manifests itself mainly in the ordering of first- and second-nearest neighbours, and correspondingly only two pair interchange energies can be derived. From a short-range order analysis and from computer simulations, also more distant neighbour pairs are often found to contribute. Their contribution to the critical ordering temperatures can easily be evaluated, using the BWG approximation, since it can be expected that in the disordered state the correlation between distant atoms is lost. For Cu–Zn alloys the third- and more-distant-neighbour pairs are not important [15, 16], and therefore the values derived from T_c should represent quite closely the correct values. This is assumed to hold also for the other noble-metal alloys. Frequently only one ordering temperature is observed, and the ratio $w^{(2)}/w^{(1)}$ or $m^{(2)}/m^{(1)}$ has to be guessed from some other information. Inden [17], when deriving the $w^{(i)}_{AB}$, assumed in this case that the same interchange energies determine also the heats of formation of the disordered alloys with respect to the same crystal structure. In this way he obtained a ratio $w^{(2)}_{AB}/w^{(1)}_{AB}$ of around 0.5. This assumption can be criticized, especially since Turchi *et al* [16] calculated a ratio $w^{(2)}_{CuZn}/w^{(1)}_{CuZn}$ of about 0.25 for Cu–Zn but nevertheless obtained a correct T_c^{β}, using the relevant κ. From a detailed analysis of the Cu–Zn, Cu–Al and Cu–Zn–Al alloys with respect to the β-phase ordering temperature and the $L2_1$ order influence on the martensitic transformation (equation (7)), it can be concluded that the ratio $w^{(2)}/w^{(1)}$ obtained by Turchi *et al* cannot be correct. It is thought that the $w^{(i)}_{AB}$ given in table 1 not only for Cu–Zn and Cu–Al but also for the other noble-metal alloys are appropriate, although their composition dependence has been neglected.

The electronegativity influences also the enthalpy of formation of the disordered phases. It is often expressed with respect to a mixture of the pure elements having the same crystal structure by a parabola

$$H_{mix} = A_{dis} c_A c_B \tag{15}$$

with A_{dis} related to the interchange energies according to [2]

$$A^{\alpha}_{dis} = 6m^{(1)}_{AB} + 3m^{(2)}_{AB}$$
$$A^{\beta}_{dis} = 4w^{(1)}_{AB} + 3w^{(2)}_{AB} \tag{16}$$

for the disordered FCC α- and BCC β-phases, respectively. The question that is to be discussed now, using the data in table 1, is the relationship between the pair interchange energies of the disordered state (equation (16)) and those derived from the order transition, for the BCC- and the FCC-based lattices. For the FCC phase the A^{α}_{dis} have been calculated from the published heats of formation [52, 53]. The linear interpolation for the pure elements in their BCC or FCC structures was done using the data for pure elements compiled by Dinsdale [54].

On comparison of $\frac{1}{6}A^{\alpha}_{dis}$ in column (9) in table 1 with the values for $m^{(1)} - 0.5m^{(2)}$ in column (5) or $m^{(1)} - 1.5m^{(2)}$ in column (6), good agreement is observed for most binary alloy systems with $e/a > 1$, i.e. for Cu–Al, Ag–Cd, Ag–Zn, Ag–Mg, Au–Cd and Au–Zn, at least within the uncertainties given in the table. The most notable exception for the FCC phase is Cu–Zn. It is clear from the results, especially for Cu–Zn and more so even for the Cu–Au and Ag–Au monovalent alloys, that the mixing enthalpy cannot always be expressed solely in terms of the same first- and second-neighbour pair interchange energies which are also those responsible for long-range order, in spite of the good correlation that is often found, as seen from table 1. In addition, the use of enthalpy differences between the phases of the pure elements can be questioned, since their atomic volumes are often very different from those obtained by extrapolation of the alloys. Therefore, the decomposition of the enthalpy of mixing into a term obtained by the linear interpolation between the elements and an electronegativity effect remains speculative until it can be clearly stated under which conditions it is valid.

As can be seen from table 1, neither the pair interchange energies nor the mixing enthalpies are solely a function of the electron concentration, as is obvious when the Cu and Ag alloys are compared with the Au alloys. It seems, however, that in spite of these considerable variations the difference between the enthalpies of formation of the α- and β-phases is largely determined by the electron concentration. As an example, Cu–Zn can be compared with Au–Cd. The entropy difference ΔS, as derived from the martensitic transformation for Au–46.5 at.% Cd, of $0.14k_B$ [55] is similar to that of the Cu alloys (equation (9)). Since it can be expected to describe well also the ΔS between α and β, as discussed earlier, an enthalpy difference of 126 K is deduced at a temperature of 900 K, the temperature at which disordered α is in equilibrium with β, which is quite similar to the enthalpy differences of Cu–Zn (160 K) and also of Cu–Al (120 K) around an electron concentration $e/a = 1.38$.

When these findings are generalized, it is suggested that the electron concentration determines the α–β relative stability and its boundary in the phase diagram whereas the energy contribution from the electronegativity is structure independent, as holds approximately within the error limits of the data for most of the alloys listed in table 1. Differences in electronegativity can manifest themselves in differences in long-range or short-range order energies, or in large differences between the heats of formation of α and β. The former case seems to be applicable to Cu–Zn, for which excess short-range order in the β-phase shifts the α–β-phase boundary to lower Zn concentrations, as discussed earlier. For Cu–Sn, on the other hand, the heats of formation in the α-phase seem to be much smaller than those of the β-phase, if judged by the high $w^{(i)}_{CuSn}$ values in table 1, and this also influences the order energies. Thus, the extension of the β-phase stability to

lower alloy concentrations observed for Cu–Zn and Cu–Sn alloys [1] can be rationalized. Whether this holds also for the Cu–In system [1] cannot be judged from the present data. Whereas in Cu–Zn the heats of mixing are larger than those which would be expected from the $m^{(i)}$ listed in table 1, for Ag–Au and more strongly for Au–Cu the opposite holds. This indicates that it is the electronegativity which makes the solid solution favourable, and that without it a phase decomposition can be expected, as occurs in fact for the Cu–Ag system, which lacks the strong electronegativity due to the Au atoms.

The prominent role of the electron concentration in the relative stability of the α-phase with respect to the β-phase is evident. It had been suggested [1] that this is due to an enhancement in the stability when the Fermi surface touches the Brillouin zone, and calculations by Evans *et al* [56] supported this hypothesis. This explanation has to be discarded, however, at least for Cu–Zn, for which sufficient data are available. The α enthalpy of formation follows a smooth parabolic relationship to 50 at.% Zn [5] and the enthalpy difference between α and β decreases continuously with increasing Zn concentration not only in the range in which the β-phase is stable at high temperatures [5] but even at lower c_{Zn}, according to the first-principle calculations by Turchi *et al* [16].

3. Martensite and equilibrium structures based on the hexagonal lattice

3.1. The 2H martensite and the influence of the lattice distortion

The formation of the 2H martensite can be described by a Bain distortion to an FCT lattice, followed by the introduction of regularly spaced stacking faults on each second close-packed plane. It is more convenient, however, to describe the transformation by a different Bain distortion parallel to the $[110]_\beta$, $[1\bar{1}0]_\beta$ and $[001]_\beta$ directions, associated with a shuffle of atoms on each second plane (figure 2). This description has the advantage that it shows more straightforwardly the relationship between the BCC and the 2H lattice, and that it does not impose additional conditions on the relation between the three Bain distortions, in contrast with those starting with an FCT lattice, for which only two independent distortions exist. Often, however, the distance between the close-packed planes in 2H does not differ within the experimental uncertainty from that of the corresponding FCT lattice, and both approaches are equivalent. One or the other is used, depending on whether the relationship between the FCT, 9R and 2H martensites is stressed, or that between 2H and the ordered BCC-based lattices is preferred, as in this paper. From figure 2 it can be seen that the 2H martensite has alternating rows of (I+II) and (III+IV) sublattice sites in the $[001]_{BCC}$ direction of the $(110)_{BCC}$ plane. This implies for the 2H martensite a deviation from the hexagonal symmetry of the basal plane. The 2H lattice therefore is orthorhombic (o). The deviation from the hexagonal symmetry can be expressed by the factor ψ:

$$a/b = \sqrt{1+2\psi^2}. \tag{17}$$

$\psi = 1$ for hexagonal symmetry, and $\psi = 1/\sqrt{2} = 0.7071$ for the {011} planes of the BCC lattice. When the 2H martensite is described by an FCT lattice with stacking faults, ψ is the tetragonality given by $\psi = (c/a)_{FCT}$.

For Cu–Zn–Al alloys a strong composition-dependent deviation of ψ from 1 has been observed for the 2H and 18R martensites, whereas the 6R martensite is nearly cubic, $c/a \simeq 1$, even after stabilization [5]. This cannot be due to an adjustment of the first- and second-neighbour atom pairs driven by the reduction in the pair interchange energies. In this case a similar distortion ψ would be expected for all three martensite structures. That

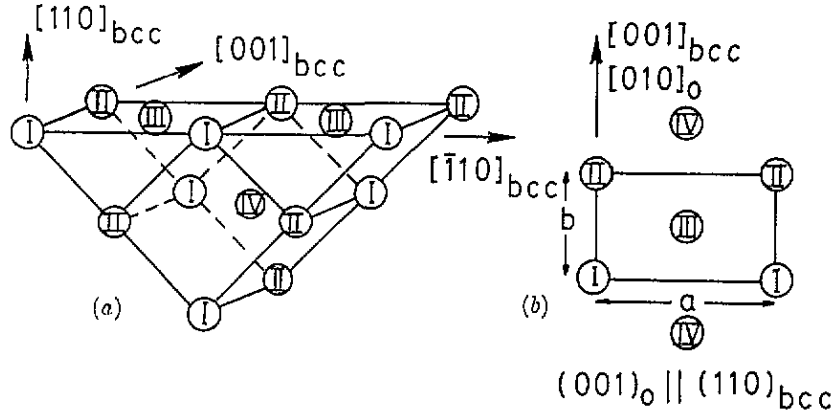

Figure 2. (*a*) BCC lattice with (110) plane exposed. (*b*) $(110)_{BCC}$ after the transformation to $(001)_o$ with the sublattice sites inherited from the BCC structure. Orthorhombic directions indicated.

order must be responsible is obvious, since in a disordered martensite the six neighbours of an atom within each compact plane are equivalent and form a hexagonal array. It has been shown, in fact, that the energy per fault in 18R—considering it as an FCT lattice with faults on each third plane—can be reduced by the distortion and depends on the FCC 6R ordering energy [57].

On generalization to other alloy systems, it is tempting to correlate a decreasing ψ with an increasing order energy of the face-centred martensite or equilibrium phase. The order energy is, according to equations (4) and (9), $H^{\alpha}_{ord} = \alpha_0 T^{\alpha}_c x_A x_B = -\alpha_0 T^{\alpha}_c c^2_B$ for a binary system with perfect B2 order. In figure 3 are plotted the ψ for Ag–Zn, Ag–Cd and Au–Cd, as taken from the literature, versus the order energy, with T^{α}_c from table 1, together with the relationship for Cu–Zn–Al at $e/a = 1.48$ [5]. The few data available indicate that there is a correlation between ψ and the α-phase ordering energy, provided that the latter rises above a critical value. ψ seems to go to a saturation value at around 0.83 for high ordering energies. This corresponds to a lattice which is intermediate in structure between BCC ($\psi = 0.707$) and hexagonal ($\psi = 1$). The decrease in ψ implies also that the amount of martensite shear decreases to about 10% at $\psi = 0.83$.

The reason for the decrease in ψ with increasing order energy will not be speculated about here. It is clear, however, that with increasing order the planes that contain the $[010]_o$ direction become more and more distinct from those containing the other close-packed directions at an angle of 120°. This provides a degree of freedom to distort the Brillouin zones in such a way that the electrons close to the Fermi surface can decrease their energy. Whether this is a reasonable explanation has to be studied in more detail.

3.2. The disordered equilibrium ξ-phase

The following observations made for 9R, 18R and 2H martensites in Cu–Zn–Al are relevant to this discussion [4]. Considering 9R, 18R and 2H as a face-centred lattice into which stacking faults are introduced on each third and second close-packed plane, a stacking fault energy can be defined, which depends strongly on ψ but extrapolates for $\psi = 1$ in the 18R martensite to that of the disordered FCC phase, at least, at $e/a = 1.48$, indicating that the interaction between the stacking faults in 18R is negligible, and that the long-range order

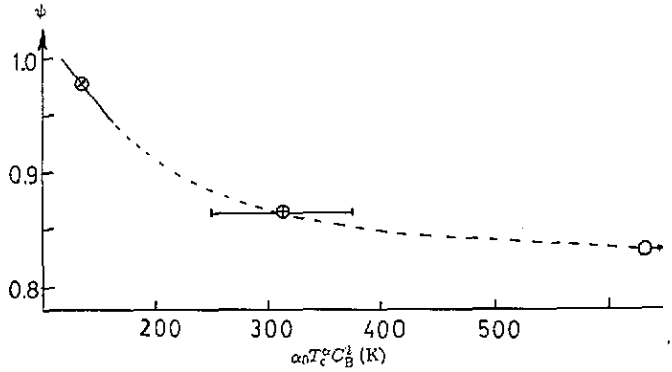

Figure 3. The distortion ψ as a function of the ordering energy in the face-centred lattice: —— near $\psi = 1$, Cu–Zn–Al with $e/a = 1.48$ [5]; ⊗, 9R Ag–38 at.% Zn [28]; ⊕, 2H Ag–47.5 at.% Cd [75]; ○, 2H Au–47.5 at.% Cd [76].

contribution in the absence of the lattice distortion is small, at least within the experimental uncertainty [57]. The stacking fault energy in the 2H martensite shows the same composition dependence as that of the 9R and 18R martensites but is 11 mJ m^{-2} higher than that of 18R, which can be considered as an unfavourable interaction between the faults in 2H, but which is absent for the more distant faults in 9R and 18R. Since this difference between 2H and 9R or 18R is independent of composition, of order energy and of the lattice distortion, it is concluded that this difference exists also for the disordered phases. This then means that, in order to describe the stability of the disordered hexagonal phase with respect to the FCC lattice at the same lattice parameter, a repulsive interaction term has to be added to the energy of a single isolated fault. The latter can be determined experimentally in the α-phase by the splitting of dislocation nodes [65]. The fact that a 9R or 18R martensite is observed in most shape memory alloys at appropriate compositions is an indication that the repulsive interaction between faults in 2H is a general phenomenon.

In the following therefore the energy difference between the FCC α-phase and the disordered hexagonal ξ-phase is considered to be the sum of the contribution of individual stacking faults, of an unfavourable interaction term and of an energy gain due to a lattice distortion. In the hexagonal lattice the distance between the atoms is determined by the atomic volume and by the ratio $(c/a)_{hex}$, i.e. by one more degree of freedom than in FCC. It is well known [1] that c/a changes with electron concentration owing to the interaction between the Brillouin zone and the Fermi surface.

In order that the disordered ξ-phase appears as an equilibrium phase, several conditions have to be met: with respect to the disordered α-phase, the repulsion between the faults has to be overcompensated by a negative stacking fault energy and/or an adequate change in $(c/a)_{hex}$ to such an extent that its Gibbs energy becomes lower than that of the two-phase mixture of the disordered α-phase and complex cubic γ-phase. With respect to the BCC phase, the enthalpy of formation of α and of ξ has to be lower than that of the disordered β-phase for Cu–Zn and Cu–Al, and therefore ξ is favoured over β at low temperatures, at which the vibrational entropy no longer contributes to the BCC structure. However, as soon as the BCC structure orders, the associated energy decrease can be sufficiently high to suppress the formation of the ξ-phase. It is not surprising therefore that ξ appears only when the ordering energy for the BCC phase is too low, either because the electronegativity (pair interchange energy) is low or because the concentration of the alloying element is low,

which occurs for higher-valency elements.

These concepts are illustrated in figure 4 for the Cu–Zn system, for which quantitative results exist. The lowering of the ξ-phase energy due to the lattice distortion has not been taken into account. The small difference between the enthalpies of α and ξ compared with the ordering energy in the BCC phase is evident. This figure can also serve as a qualitative guide to rationalize the formation of ξ in Ag–Cd in a limited temperature range between 513 and 713 K. The B2 phase becomes more stable than ξ even when it is only partially ordered and reappears again at low temperatures. For this reason, the unknown critical temperature T_c^{β} should not be too high, and its location in the middle of the ξ-phase stability range seems reasonable.

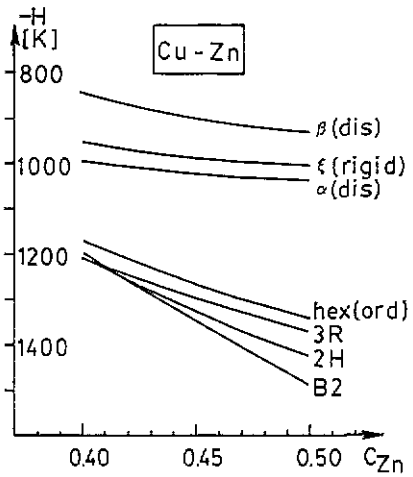

Figure 4. Heats of formation as a function of Zn concentration for Cu–Zn for disordered BCC (β(dis)) from [5], for disordered FCC (α(dis)) and disordered hexagonal without change in $(c/a)_{hex}$ (ξ(rigid)), for ordered hexagonal with $\psi = 1$ (hex(ord)), for 3R and 2H martensites, for 3R with $(c/a)_{FCT} \simeq 1$, for 2H with variable $\psi < 1$ and for B2 ordered BCC. The difference 3R – hex(ord) which is the same as α(dis) – ξ(rigid) is from [4], α(dis) – β(dis) from [5], and 3R, 2H, B2 from [3, 4].

Figure 4 also shows that the hexagonal phase can become more stable if it orders. This is expected to occur only if also the FCC phase has a sufficiently high ordering energy; additional contributions could be due to a change in $(c/a)_{hex}$ and to the formation of long-period superlattices [1]. Au–Cd and Au–Zn with their high T_c^{α} can be a case in point.

4. The Ni–Al martensite

The Ni–Al and Ni–Ti alloys have been the subject of considerable interest owing to their shape memory behaviour associated with the martensitic transformation. Ni–Ti has a lattice distortion which is different from those discussed in this paper [7] and therefore will not be considered further. The Ni–Al alloys, on the other hand, transform martensitically in a way similar to those of the noble-metal alloys. In addition, the ordering tendencies are increased, which brings the Ni–Al alloys close to true intermetallic compounds. For these reasons it is appropriate to compare the martensitic transformations in the noble-metal alloys with that of Ni–Al. The Ni–Al alloys have also found applications for their mechanical properties as

superalloys, and thus information from the martensitic transformation may become relevant also for the dislocation behaviour in these alloys [66].

The martensite has an FCT twinned structure at and below 36.6 at.% Al, and a 7R lattice above this composition [67–69]. The FCT lattice has a strong tetragonal distortion of $(c/a)_{FCT} = 0.85$ for 36.6 at.% Al [67] and, for the 7R, $\psi = 0.84$ is obtained for 37.5 at.% Al [68]. This distortion is similar to that expected from the curve in figure 3 extrapolated to the ordering energy of Ni_3Al. Whether this coincidence is accidental or points to some common features is not clear. It should be emphasized, however, that this strong tetragonal distortion cannot be explained by the ordering of hard spheres with different radii. A linear extrapolation of the atomic volumes v_a to pure Ni and Al leads to a relative difference $[v_a(Al) - r_a(Ni)]/r_a(Ni) = 13.7\%$, corresponding to a radius difference $r_{Al}/r_{Ni} = 4.4\%$, which would lead to $(c/a)_{FCT}$ considerably closer to 1.

From short-range order studies on Ni–10 at.% Al [71, 72] and from *ab-initio* calculations [73] it has become evident that more distant atom pairs contribute considerably to the order energy. Therefore, it is not possible to relate the order temperature which has been measured [70] by a factor $\alpha_0 = 4.3$ to the pair interchange energies. Since it can be expected that the correlation between more distant atom pairs disappears largely in the disordered state above T_c^{α}, their contribution can easily be incorporated using the BWG approximation [66, 71].

The ordering energies for B2 and $L1_0$ at 50 at.% Ni have been calculated [73] and can be compared with those which would be expected from the martensitic transformation. At $c_{Al} = 0.388$, $M_s = 0$ K and, according to equations (5) and (6), the energy difference between the disordered FCC and BCC is equal to the ordering energy. Using a composition dependence of the ordering energy proportional to c_{Al}^2 (equations (5) and (6)) and taking the calculated value of 1952 K at 50 at.% Al for the difference between the order energies of B2 and $L1_0$ [73], a value of 1175 K is obtained for $H_{dis}^{\beta} - H_{dis}^{\alpha}$ at 38.8 at.% Al. This is a factor of 10 higher than that for the noble-metal alloys. It is very doubtful whether this is realistic. If we assume that $H_{dis}^{\beta} - H_{dis}^{\alpha} = 115$ K, as for Cu–Al, the difference in order energy at 50 at.% Zn would also be reduced by a factor of 10 [66].

5. Pre-martensitic phenomena and surface martensite

Recently, attention has been focused on pre-martensitic phenomena, such as the tweed contrast, which is observed in the electron microscope. Robertson [58] has suggested that, in order to exhibit strong tweed contrast, the alloy must possess a high elastic anisotropy, a high ordering temperature and a large deviation from the stoichiometric composition. The importance of these three factors can easily be rationalized. A high ordering energy corresponds according to figure 3 to a low ψ and thus to a decrease in martensite shear. The lower the martensite shear, the less distortion is required in the surrounding BCC matrix to create a martensite embryo. Even if the martensite is not yet stable at temperatures close to but above A_f, the thermal energy can be sufficient to create embryos of martensite-like structures by fluctuations, if also the elastic constants, especially c', are small, which corresponds to a high elastic anisotropy. When the formation of the martensite is too unfavourable energetically, the fluctuations disappear. Since M_s decreases generally with increasing alloy concentrations towards the stoichiometric composition, the tweed contrast should also decrease. Thus, for Cu–Zn, Cu–Al–Ni and Cu–Zn–Al there is a medium tweed contrast level [58], which moreover is limited to the surface regions [59] for Cu–Zn–Al provided that no surface martensite forms, whereas for Au–47.5 at.% Cd and Ni–Al away from 50 at.% Al it is strong, as can be expected.

It should be mentioned in passing that the enhanced vibration amplitude near the surface in Cu–Zn–Al should increase the vibrational entropy of the BCC phase, and consequently decrease M_s. It has been observed instead that the martensite formation is enhanced in surface regions of about 10 nm thickness with the appropriate orientation [60–62], leading to a surface M_s about 500 K above that for the bulk. Thus, this change in M_s seems not to be related to a tweed-type lock-in of the thermal fluctuations near the surface. It is more likely that, during the oxidation of the surface, vacancies are injected, which enhance diffusion [63] and produce stabilization of the martensite during its formation, as in bainite-type transitions. The stabilization of the martensite can lead to considerable changes in M_s also in the bulk [64].

6. Summary

Based on recent results for Cu–Zn–Al [3–5] an evaluation of the contributions to the stabilities of martensitic and equilibrium phases is made for other noble-metal alloys and for Ni–Al, using data from the literature which are often not complete. It is hoped, however, that the speculative part of this work can be reduced in the future by more experimental results.

(1) The face-centred 3R or 6R martensites with inherited B2 or $L2_1$ order can be well related energetically to the disordered α FCC and β BCC equilibrium phases and to the difference in long-range order contribution which is given by the pair interchange energies or equivalently by the critical ordering temperatures. The long-range order can shift M_s considerably with respect to the equilibrium temperatures between the α- and β-phases.

(2) In the 9R, 18R and 2H martensites of many noble-metal alloys an important contribution to the stability is due to a distortion of the basic cubic or hexagonal lattice. This complicates the comparison with the disordered hexagonal ξ-phases which are observed as equilibrium phases in many noble-metal alloys. The distortion depends on the ordering energy in the α-phase. With increasing α-phase order the 2H martensite becomes more BCC like, and the corresponding martensite shear decreases. This holds also for the Ag and Au alloys and probably influences the formation of tweed phenomena, which have been studied by transmission electron microscopy.

(3) A comparison of the data for the different noble-metal alloys permits one to evaluate the influence of the lattice parameters, electron concentration and electronegativity on the stability of the Hume-Rothery noble-metal alloys.

(4) The martensites in Ni–Al show many aspects similar to those of the noble-metal alloys. On the other hand they are representative of the transition towards true intermetallics.

Acknowledgments

This work has been supported by grant S-41/1991 from DGICYT of Spain during a sabbatical stay at the UPC, and by the Consejo Nacional de Investigaciones Cientificas y Tecnicas of Argentina.

References

[1] Barrett C S and Massalski T B 1966 *Structure of Metals* 3rd edn (New York: McGraw-Hill)
[2] Ahlers M 1986 *Prog. Mater. Sci.* **30** 135
[3] Pelegrina J L and Ahlers M 1992 *Acta Metall. Mater.* **40** 3205
[4] Ahlers M and Pelegrina J L 1992 *Acta Metall. Mater.* **40** 3213
[5] Saule F, Ahlers M, Kropff F and Rivero E B 1992 *Acta Metall. Mater.* **40** 3229
[6] Warlimont H and Delaey L 1974 *Prog. Mater. Sci.* **18** 1
[7] Nishiyama Z 1978 *Martensitic Transformations* (London: Academic)
[8] Rapacioli R and Ahlers M 1979 *Acta Metall.* **27** 777
[9] Planes A, Romero R and Ahlers M 1990 *Acta Metall. Mater.* **38** 757
[10] Ahlers M 1980 *Z. Metallk.* **71** 704
[11] Romero R and Ahlers M 1989 *J. Phys.: Condens. Matter* **1** 3191
[12] Inden G 1975 *Z. Metallk.* **66** 577
[13] Mohri T, Sanchez J M and de Fontaine D 1985 *Acta Metall.* **33** 1171
[14] Gerold V and Kern J 1987 *Acta Metall.* **35** 393
[15] Reinhard L, Schönfeld B, Kostorz G and Bührer W 1990 *Phys. Rev.* B **41** 1727
[16] Turchi P E A, Sluiter M, Pinski F J, Johnson D D, Nicholson D M, Stocks G M and Staunton J B 1991 *Phys. Rev. Lett.* **67** 1779
[17] Inden G 1975 *Z. Metallk.* **66** 648
[18] Iwasaki H, Hirabayashi M, Fujiwara K, Watanabe D and Gava S O 1960 *J. Phys. Soc. Japan* **15** 1771
[19] Pops H and Massalski T B 1965 *Trans. AIME* **233** 728
[20] Ridley N and Pops H 1970 *Metall. Trans.* **1** 2867
[21] Iwasaki H 1962 *J. Phys. Soc. Japan* **17** 1620
[22] Nakanishi N, Murakami Y and Kachi S 1968 *Scr. Metall.* **2** 673
[23] Nakanishi N, Murakami Y and Kachi S 1971 *Scr. Metall.* **5** 433
[24] Bowe R C and Muldawer L 1979 *Proc. Int. Conf. on Martensitic Transformations* (Cambridge: MA: MIT Press) p 265
[25] Miura S, Maeda S and Nakanishi N 1974 *Phil. Mag.* **30** 565
[26] Brookes M E and Smith R W 1969 *Scr. Metall.* **3** 667
[27] Iwasaki H, Fujimura T, Ichikawa M, Endo S and Wakatsuki M 1985 *J. Phys. Chem. Solids* **46** 463
[28] Kubo H, Shimizu K and Wayman C M 1977 *Metall. Trans.* A **8** 493
[29] Clarebrough L M, Hargreaves M E and Loretto M H 1963 *J. Aust. Inst. Met.* **8** 308
[30] Matsuo S and Clarebrough L M 1963 *Acta Metall.* **11** 1195
[31] Rivlin V G, Hume-Rothery W and Ryder B 1962 *Acta Metall.* **10** 1143
[32] Hirabayashi M, Hiraga K, Yamaguchi S and Ino N 1969 *J. Phys. Soc. Japan* **27** 80
[33] Hirabayashi M, Yamaguchi S, Hiraga K, Ino N, Sato H and Toth R S 1970 *J. Phys. Chem. Solids* **31** 77
[34] Sakamoto H, Tsuzuki H and Shimizu K 1990 *Mater. Sci. Forum* **56–8** 305
[35] Waldman J and Bever M B 1972 *Metall. Trans.* **3** 1007
[36] Masson D B 1960 *Trans. AIME* **218** 94
[37] Krishan R V and Brown L C 1973 *Metall. Trans.* **4** 1017
[38] Tong H C and Wayman C M 1973 *Scr. Metall.* **7** 215
[39] Walker C B and Marezio M 1963 *J. Appl. Phys.* **34** 1443
[40] Tadaki T, Nagaura T and Shimizu K 1978 *Scr. Metall.* **12** 453
[41] Rothwarf F and Muldawer L 1962 *J. Appl. Phys.* **33** 2531
[42] Nakanishi N, Takano M, Morimoto H, Miura S and Hori F 1978 *Scr. Metall.* **12** 79
[43] Ziesemer K and Schüle W 1985 *Acta Metall.* **33** 587
[44] Saburi T and Wayman C M 1965 *Trans. AIME* **233** 1372
[45] Swann P R and Warlimont H 1963 *Acta Metall.* **11** 511, 1099
[46] Nishiyama Z, Morikawa H and Shimizu K 1967 *Japan. J. Appl. Phys.* **6** 815
[47] Miura S, Morita Y and Nakanishi N 1975 *Shape Memory Effects in Alloys* ed J Perkins (New York: Plenum) p 389
[48] Kubo H, Hamabe A and Shimizu K 1976 *Scr. Metall.* **10** 547
[49] Arias D and Kittl J 1969 *Trans. AIME* **245** 182
[50] Hawbolt E B and Massalski T B 1971 *Metall. Trans.* **2** 1771
[51] Pfeiler W 1988 *Acta Metall.* **36** 2417
[52] Predel B 1990 *Landolt–Börnstein New Series* Group IV, vol 5a (Berlin: Springer)
[53] Hultgren R, Orr R L, Anderson P D and Kelley K K (ed) 1963 *Selected Values of Thermodynamic Properties of Metals and Alloys* (New York: Wiley)

[54] Dinsdale A T 1991 *Calphad* **15** 317
[55] Miura S, Mori T, Nakanishi N, Murakami Y and Kachi S 1976 *Phil. Mag.* **34** 337
[56] Evans R, Lloyd P and Mujibur Rahman S M 1979 *J. Phys. F: Met. Phys.* **15** 1939
[57] Ahlers M 1992 *Phys. Status Solidi* b **172** 65
[58] Robertson I M 1990 *Mater. Sci. Forum* **56–8** 59
[59] Van Tendeloo G, Chandrasekaran M and Lovey F C 1986 *Metall. Trans.* A **17** 2153
[60] Lovey F, Chandrasekaran M, Rapacioli R and Ahlers M 1980 *Z. Metallk.* **71** 37
[61] Lovey F C, Chandrasekaran M and Ahlers M 1981 *Z. Metallk.* **72** 43
[62] Lovey F C and Chandrasekaran M 1983 *Acta Metall.* **31** 1919
[63] Lovey F C, Ferron J, de Bernardez L S and Ahlers M 1983 *Scr. Metall.* **17** 501
[64] Abu Arab A and Ahlers M 1988 *Acta Metall.* **36** 2627
[65] Gallagher P C J 1970 *Metall. Trans.* **1** 2429
[66] Ahlers M 1993 *Centro Atómico Bariloche Informe Técnico CNEA-CAB* 3016
[67] Chakravorty S and Wayman C M 1976 *Metall. Trans.* A **7** 555
[68] Noda Y, Shapiro S M, Shirane G, Yamada Y, Fuchisaki K and Tanner L E 1990 *Mater. Sci. Forum* **56–8** 299
[69] Murakami Y, Otsuka K, Hanada S and Watanabe S 1992 *Mater. Trans. Japan Inst. Met.* **33** 282
[70] Cahn R W, Siemers P A, Geiger J E and Bardhan P 1987 *Acta Metall.* **35** 2737
[71] Chassagne E, Bessiere M, Calvayrac Y, Cenedese P and Lefebre S 1989 *Acta Metall.* **37** 2329
[72] Klaiber F, Schönfeld B and Kostorz G 1987 *Acta Crystallogr.* A **43** 525
[73] Sluiter M, Turchi P E A, Pinski F J and Stocks G M 1992 *Mater. Sci. Eng.* A **152** 1
[74] Rapacioli R and Ahlers M 1977 *Scr. Metall.* **11** 1147
[75] Tadaki T, Hamada S and Shimizu K 1977 *Trans. Japan Inst. Met.* **18** 135
[76] Morii K, Ohba T, Otsuka K, Sakamoto H and Shimizu K 1991 *Acta Metall. Mater.* **39** 2719
[77] Zener C 1948 *Elasticity and Anelasticity of Metals* (Chicago: University of Chicago Press)
[78] Massalski T B and Mizutani U 1978 *Prog. Mater. Sci.* **22** 151